THE ELASTIC SCATTERING OF 1.1 MEV GAMMA-RAYS FROM LEAD AT 30°

A Thesis

submitted in partial fulfilment of

the requirements for the degree of

Master of Science

at the

University of Manitoba

by

Gerald Hardie

August, 1956.

ABSTRACT

A summary of the pertinent theoretical data available on the elastic scattering of gamma-rays is presented. Some discussion is devoted to an experimental technique suitable for detecting the small angle elastic scattering of gamma-radiation. This thesis also reports an experiment carried out to determine the differential elastic cross section for 1.12 Mev. gamma-rays scattered from lead at an angle of $33^{\circ} \pm 4^{\circ}$. The cross section obtained was 21.2 ± 1.4 millibarns/steradian. This cross section is compared with the results of other workers.

ACKNOWLEDGMENTS

The author wishes to express his sincere thanks to Dr. K.G. Standing for his guidance throughout the project; to Dr. S.M. Neamtan for many helpful discussions on the theoretical aspects; and to Mr. C. Kubin for his aid with the mechanical work.

The receipt of a bursary from the National Research Council of Canada, as well as their financial support of the project, is gratefully acknowledged.

TABLE OF CONTENTS

LIST OF FIGURES

I INTRODUCTION

Physical theories are formulated in order to explain experimental facts. These theories are eventually discarded, modified, or their ranges of validity realized as new experimental facts are uncovered and previous methods are refined. In addition to explaining existing experimental data a new theory usually predicts the existence of hitherto unexpected phenomena. An important part of experimental physics is determining the validity of a new theory by investigating these phenomena.

Classical electromagnetic theory has been succeeded by quantum electrodynamics. Quantum electrodynamics predicts phenomena which, according to classical electromagnetic theory, cannot exist. One such prediction is the scattering of light by light (1). Because of their linearity the classical electromagnetic equations cannot predict this phenomenon. Although the cross section is so small that experimentalists cannot hope to observe this effect in a crossed beam experiment. Delbrück (2) suggested that the scattering of gamma-radiation by the Coulomb field of the nucleus, a formally equivalent process, might be detectable. The latter process is usually called Delbrück scattering or nuclear potential scattering.

The problem of Delbrück scattering is difficult both theoretically and experimentally. Attempts have been made to obtain experimentally the Delbrück differential scattering cross section by measuring the total elastic scattering cross section and subtracting from it the sum of the theoretically computed differential cross sections arising from all other types of elastic scattering. Although the angular distribution of gamma-radiation scattered by the Coulomb field is unknown it seems likely that there will be some peaking in the forward direction. The experimental differential elastic scattering cross section is therefore of particular interest at small angles. Also Rayleigh scattering (elastic scattering by tightly bound electrons) is predominantly in the forward direction and falls off very rapidly with increasing angle. However, at small angles a photon scattered by the much more likely Compton process has an energy only slightly smaller than the energy of an incident photon. Clearly the most important problem experimentally is to resolve the elastic scattered and Compton scattered gamma-rays.

Several workers (3), (4) and (5) have attacked this problem. These workers have claimed evidence for the existence of Delbrück scattering. However, Mann (6), in a recent paper, has pointed out that no unambiguous evidence exists for the existence of potential scattering because of the uncertainty in the accuracy of the theoretical results for Rayleigh scattering. From the results of these workers it is evident that better experimental measurements and better theoretical results must be obtained before the question of Delbrück scattering can be satisfactorily answered.

This thesis reports an attempt made to obtain more accurate experimental measurements at a scattering angle of 30^{o}. The method used was that indicated by Standing and Peelle (7).

This method is very suitable for small scattering angles. Although measurements are reported for a single scattering angle it is hoped that this method will be employed at smaller angles in the near future.

II THEORETICAL CONSIDERATIONS

A. Incoherent Scattering and Complete Absorption

The attenuation of a beam of gamma-radiation as it passes through matter occurs by a number of elementary processes. A gamma-ray, upon interaction with a particle or field, may undergo complete absorption, inelastic (incoherent) scattering, or elastic (coherent) scattering. This section is devoted to a brief discussion of the main processes involving complete absorption or inelastic scattering. These are the photoelectric effect, pair production, and Compton scattering.

In the photoelectric effect the gamma-ray is completely absorbed. An electron (usually a K-electron) is freed and generally given considerable kinetic energy. This effect predominates in the energy region below 0.1 Mev., especially for high Z materials. The cross section decreases very rapidly with increasing energy. For energies greater than 0.1 Mev. the cross section is roughly proportional to Z^5. For energies less than 0.5 Mev. the electrons are ejected primarily at right angles to the incident beam but the forward direction becomes predominant at higher energies. One result of the photoelectric effect is the production of bremsstrahlung by the photoelectrons as they are stopped in the target. The energy range of the bremsstrahlung may extend almost up to the energy of the incident radiation.

The only other important process which causes complete absorption of the initial photon is pair production. According to the Dirac ''Hole Theory'' the incident gamma-ray causes an electron to undergo a transition from a negative energy state to a positive energy state. The ''hole'' in the electron vacuum is interpreted as a positron and, therefore, an electron-positron pair is created in order for this process to occur the incident photon must have an energy of at least 2 mc^2 and a third particle (usually a nucleus) must be present in order to have energy and momentum conservation.

Compton scattering is the major inelastic scattering process which affects the experiment discussed in this thesis. A gamma-ray interacts with a loosely bound electron. The gamma-ray is scattered with decreased energy, the energy difference being employed to free the electron and provide it with kinetic energy. Using the laws of conservation of energy and momentum, the energy ($h\nu'$) of the scattered radiation, in terms of the scattering angle (θ), is easily found to be (8)

$$h\nu' = \frac{h\nu}{1 + \frac{h\nu}{mc^2}(1 - \cos\theta)}$$

with h representing Planck's constant, ν' the frequency of the scattered photon, ν the frequency of the incident photon, c the velocity of light, and m the rest mass of the electron.

In addition to the energy of the scattered photon the angular distribution is also of interest. This information is supplied by the Klein-Nishina differential scattering cross section. Averaging over all angles of polarization of the incident radiation and summing over the angles of polarization of the scattered radiation the Klein-Nishina formula becomes (9)

$$\left(\frac{d\sigma}{d\Omega}\right)_\theta = \frac{r_0^2(1+\cos^2\theta)}{2}\,\frac{1}{[1+\frac{h\nu}{mc^2}(1-\cos\theta)]^2}\left\{1+\frac{(\frac{h\nu}{mc^2})^2\,(1-\cos\theta)^2}{(1+\cos^2\theta)[1+\frac{h\nu}{mc^2}(1-\cos\theta)]}\right\}$$

with $\left(\frac{d\sigma}{d\Omega}\right)_\theta$ representing the differential scattering cross section at an angle θ, and r_0 representing the classical electron radius $\frac{e^2}{mc^2}$. The differential cross section is measured in units of cm^2/steradian/scattering centre.

The above discussion has been brief as the material is easily found in standard reference works (10). However, the subject of elastic scattering has not been studied as thoroughly and the available information is not easily found. Therefore, the next section, devoted to elastic scattering, is more detailed.

B. Coherent Scattering

In this section a summary is given of the theoretical work done on the elastic scattering of gamma-radiation. The processes discussed are nuclear Thomson scattering, Rayleigh scattering, nuclear resonance scattering, and Delbruck scattering.

The derivation of the cross section for the scattering of electromagnetic radiation by a free electron yields, on the basis of classical electromagnetic theory (11),

$$\left(\frac{d\sigma}{d\Omega}\right)_\theta = \frac{r_0^2}{2}(1+\cos^2\theta)$$

The symbol $\left(\frac{d\sigma}{d\Omega}\right)_\theta$ represents the differential scattering cross section for a scattering angle of θ, and r_0 represents the classical electron radius $\frac{e^2}{mc^2}$. A quantum electrodynamical treatment of the scattering of electromagnetic radiation by a free electron yields the Klein-Nishina formula. However, in the non-relativistic case†, the Klein-Nishina formula yields the Thomson cross section. The classical Thomson formula is therefore correct in a non-relativistic situation.

The scattering of radiation of a few Mev. by the nuclear charge is such a non-relativistic case since the rest mass of the nucleus will be much greater than a few Mev. The classical Thomson formula can therefore be applied. However, in this case, the classical electron radius must be replaced by $\frac{(ze)^2}{Mc^2}$, M representing the nuclear mass. The differential cross section for nuclear Thomson scattering is therefore

$$\left(\frac{d\sigma}{d\Omega}\right)_\theta = \frac{Z^4 e^4}{2M^2c^4}\left(1 + \cos^2\theta\right)$$

Rayleigh scattering is well known in the X-ray region, being the coherent scattering responsible for X-ray diffraction phenomena. This is a process whereby a bound electron scatters an incident photon. The electron remains in its initial state and the atom as a whole recoils. The cross section for Rayleigh scattering has not yet been computed completely. The results presently available are the form factor†† calculations. The cross

---

† The non-relativistic case occurs whenever the energy of the incident photon is much smaller than the rest mass of the scattering centre.

†† The form factor can be introduced in the following manner. Consider an atom scattering radiation by means of its tightly bound electrons. The scattering amplitude is written as the classical Thomson scattering amplitude multiplied by a factor called the form factor. For a clear discussion of this factor and its role in X-ray diffraction see Chapter III of R.W. James' The Optical Principles of the Diffraction of X-rays (Bell).

section is written in the form (12),

$$\left(\frac{d\sigma}{d\Omega}\right)_\theta = \frac{r_0^2}{2}\left(1+\cos^2\theta\right)\left|f(\Delta q)\right|^2$$

where Δq represents the change in momentum of the photon scattered and $f(\Delta q)$ is the form factor. The form factor is given by

$$f(\Delta q) = \left(0\left|\sum_{j=1}^{Z} e^{\frac{i}{\hbar}\Delta q\cdot r_j}\right|0\right)$$

r_j representing the position of the j[th] electron (with respect to the nucleus) and 0 denoting the ground state of the atom.

Two aspects of these form factor calculations must be discussed; the work done to compute the form factor and the errors involved in the form factor calculations. First the computations are discussed. Franz (13) make the first form factor calculations in the gamma-ray region. To compute the form factor he used the Fermi-Thomas electron distribution. Bethe† computed the form factor using Dirac wave functions for the K-electrons and ignoring the other electrons. Nelms and Oppenheim (12) have used the Hartree self-consistent field as a basis for their form factor calculations.

The neglect of all electrons except those in the K-shell, in computations involving Dirac wave functions, introduces some error. Woodward (15) and also Rohrlich and Rosenzweig (14) have considered the L-shell contribution and have shown that, when Δq is large, it will be approximately an eighth as large as that from the K-shell.

---

† Private communication to Levinger. Reference (14).

All the form factor calculations suffer from the fact that the non-relativistic assumption $\Delta q \ll mc$ must be employed. Attempts have been made to extend the form factor calculations into the relativistic and near relativistic regions, that is, regions in which $\Delta q \ll mc$ is no longer true. Levinger (14) obtained a correction factor for the form factor calculations when the change in photon momentum is in the near relativistic region. His work is valid only for small Z. He shows that in this region the correction to the form factor is small, being of the order $\frac{Z}{137}\left(\frac{\Delta q}{mc}\right)$.

In addition Levinger also reported the results of a numerical computation for the scattering of gamma-rays from tin. Dirac wave functions were used and the K electrons alone were considered. For $\frac{\Delta q}{mc} = 1.5$ the results indicate an increase of 25% over the form factor prediction.

In the intermediate states† of Rayleigh scattering the electron is bound but in all form factor calculations this binding is neglected. Levinger, in his work in the near-relativistic region, also neglects this binding. The effect of this neglect has been studied by Brown and Woodward (15). They show that binding in the intermediate states can give a contribution as large as the form factor itself provided Δq is large. Their work is only valid for light atoms.

† Rayleigh scattering can be considered as a two stage process. A transition is made from the initial state to some state called the intermediate state, and then from this state to the final state.

The form factor calculations consider only dispersive scattering, that is, scattering in which the intermediate states are virtual. However, there is some contribution from absorptive scattering. In absorptive scattering the intermediate states are real. This process can be considered as a real photoelectric effect followed by the capture of the ionized electron. Greifinger, Levinger, and Rohrlich (16) have considered the special case of the 180° scattering of 1.33 Mev. gamma-rays by the K-shell of lead atoms. The dispersive contribution was shown to be about one-half, and the absorptive contribution about one-third, of the scattering predicted by the form factor computation (Bethe's). The absorptive contribution is probably smaller for lighter elements and smaller photon momentum changes.

Since all the corrections to the form factor calculations are interdependent it is difficult to predict their cumulative effect. However, the magnitude of the corrections do show that the accuracy of the theoretically predicted Rayleigh cross section is in considerable doubt. At present Brown et al (17), (18), at Birmingham are performing exact computations for selected scatterers and photon energies. It is hoped that they will soon be making calculations in the 1 Mev. region for heavy elements.

Rayleigh scattering takes place mainly in the forward direction. According to Franz' (13) calculation more than three-quarters of the radiation is scattered within a characteristic angle θ_0 given by

$$\theta_0 = 2 \sin^{-1} \left[Z^{1/3} \frac{m_0 c^2}{E} 2.6 \times 10^{-2} \right]$$

As an example, for 1.12 Mev. gamma-rays scattered by lead, θ_0 is about 6°. Franz also showed† that the ratio of the total Rayleigh cross section to the total Compton cross section is approximately given by

$$\frac{\sigma_R}{\sigma_c} = 4.2 \times 10^{-5} Z^{5/3} \frac{m_o c^2}{E}$$

For lead and 1.12 Mev. gamma-rays this gives $\frac{\sigma_R}{\sigma_c} = 2.99 \times 10^{-2}$. Rayleigh scattering is coherent and in phase with the previously discussed nuclear Thomson scattering (19). At small angles and in the energy range of a few Mev. Rayleigh scattering is the predominant type of elastic scattering.

Nuclear resonance scattering is a third elastic scattering process. If an incident gamma-ray has an energy equal to the energy difference between the ground state and an excited state of a nucleus, it may excite the nucleus. In decaying back to the ground state a gamma-ray is emitted with an energy equal to the energy of the incident photon. Schemes to detect nuclear resonance scattering utilize a scatterer consisting (in part at least) of atoms identical with those whose gamma decay gives rise to the incident radiation. If the source nuclei and scattering nuclei are different it is extremely unlikely that the incident gamma-ray will be near a resonance. There will be some resonant scattering from the ''tails'' of the resonance curve of the various nuclear levels. However, Levinger (20) has shown that in the energy region about 1 Mev. the total contribution from this type of scattering is negligible compared to the contribution from nuclear Thomson scattering. Nuclear resonance

---

† There is, however, an error in Franz' work. See reference (12). The corrected formula is given above.

scattering is coherent with the previous by discussed nuclear Thomson scattering and Rayleigh scattering (19).

Finally Delbrück scattering will be considered. This is the scattering of electromagnetic radiation by virtual pair production in the Coulomb field of the nucleus. This type of scattering is of interest since it is an effect due to vacuum polarization (21). Study of the similar problem of the scattering of light by light indicated that the cross sections were too small (22) for the effect to be found experimentally. Since Delbrück scattering is a formally equivalent process attempts have been made to obtain some estimate of its cross section and angular distribution.

The computation of Delbrück scattering is so difficult that very little successful work has been accomplished. Rohrlich and Gluckstern (23) and also Toll (24) have computed the cross section in the forward direction. For forward scattering the cross section increases rapidly with photon energy. With a lead scatterer the differential scattering cross section in the forward direction is 0.591 millibarns/steradian for an incident energy of 1.33 Mev. and 1.82 kilobarns/steradian for an incident energy of 200 Mev. The only other important work done in this field was by Bethe and Rohrlich (25). They compute the angular distribution at small angles. Their work is valid for photon energies large compared to the electron rest energy. A strong peaking in the forward direction is indicated by their results.

This section has summarized the facts about elastic scattering which are of significance for the experiment to be described. In particular nuclear Thomson and resonance scattering are thought to be understood very well. Rough calculations exist for Rayleigh scattering but the accuracy of the theoretical results are uncertain. At present more exact computations for Rayleigh scattering are being performed at Birmingham. Very little work has been done on Delbruck scattering and theoretical knowledge exists only for small angle scattering.

III THE EXPERIMENT

A. Experimental Technique

It is assumed that the reader is familiar with the simple scintillation spectrometer. The term ''photopeak'' will be applied to that part of the scintillation spectrum corresponding to the crystal capturing the total energy of the impinging gamma-ray. In the experiment under consideration gamma-rays from a $_{30}Zn^{65}$ source were scattered by a lead target. A NaI (Tl) crystal detected the gamma-rays scattered through an angle of about 30^{o}. The crystal was shielded against normal room background and direct radiation from the source by the arrangement shown in Figure 1.

The step arrangement in the shielding between source and crystal is to prevent ''slit scattering''. This type of scattering occurs when a gamma-ray scatters from a part of the shielding and can reach the crystal without penetrating much lead. For instance, if the steps were not present, point A in Figure 1 would give rise to this type of scattering. The target stand is made of balsawood and will not give appreciable scattering.

In the spectrum of the scattered radiation there are two photopeaks. One arises from the elastically scattered gamma-radiation and the other from the Compton scattered gamma-rays. As was previously mentioned the main experimental difficulty is to resolve these photopeaks. The technique used to overcome this difficulty will now be summarized briefly. For more details the

ONE-THIRD OF FULL SCALE

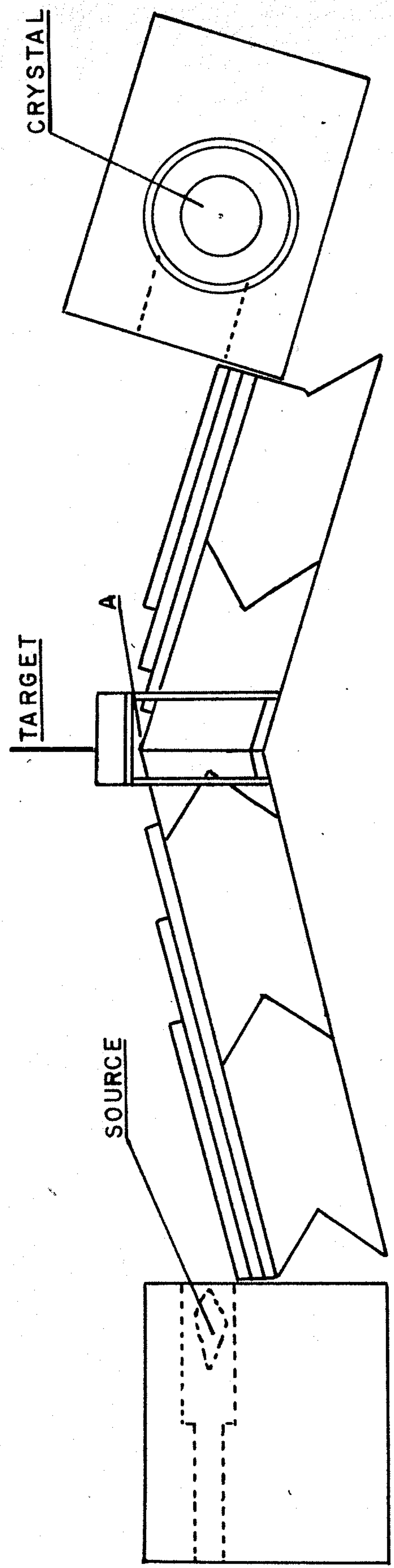

FIGURE I.

paper of Standing and Peelle (8) should be consulted.

The basis of the technique employed will be discussed with the aid of a typical situation. Figure 2 (a) shows two photopeaks lying close together. The full line, which is the sum of the distributions A and B, indicates the spectrum which would be obtained using a simple scintillation spectrometer. From this spectrum it is not clear that two photopeaks are present.

Now two photomultipliers observe events in the same crystal. Each photomultiplier has its own amplifying system. One photomultiplier and its system R is again used to record the spectrum. The other photomultiplier and its system G is used to ''gate'' the system R which is recording the spectrum:- The ''gating'' is done in the following manner. A pulse appears at the output of the ''gating'' system G whenever it receives a pulse larger than K, K being indicated in Figure 2 (b). The systems are so arranged that an output pulse from the recording system R will be registered only when a pulse appears at the output of the ''gating'' system G. The effect of this on the two distributions (A and B) is now investigated. Consider the distribution marked A. Since the photomultiplier statistics (which causes the broadening of the lines) are independent for the two photomultiplier tubes the distribution will remain centred about the same point. However, the system G will only allow a certain number of counts to be registered. The ratio of the number of counts recorded to the actual number of counts (in the distribution A) will be the same as the ratio of the shaded area to the total area under

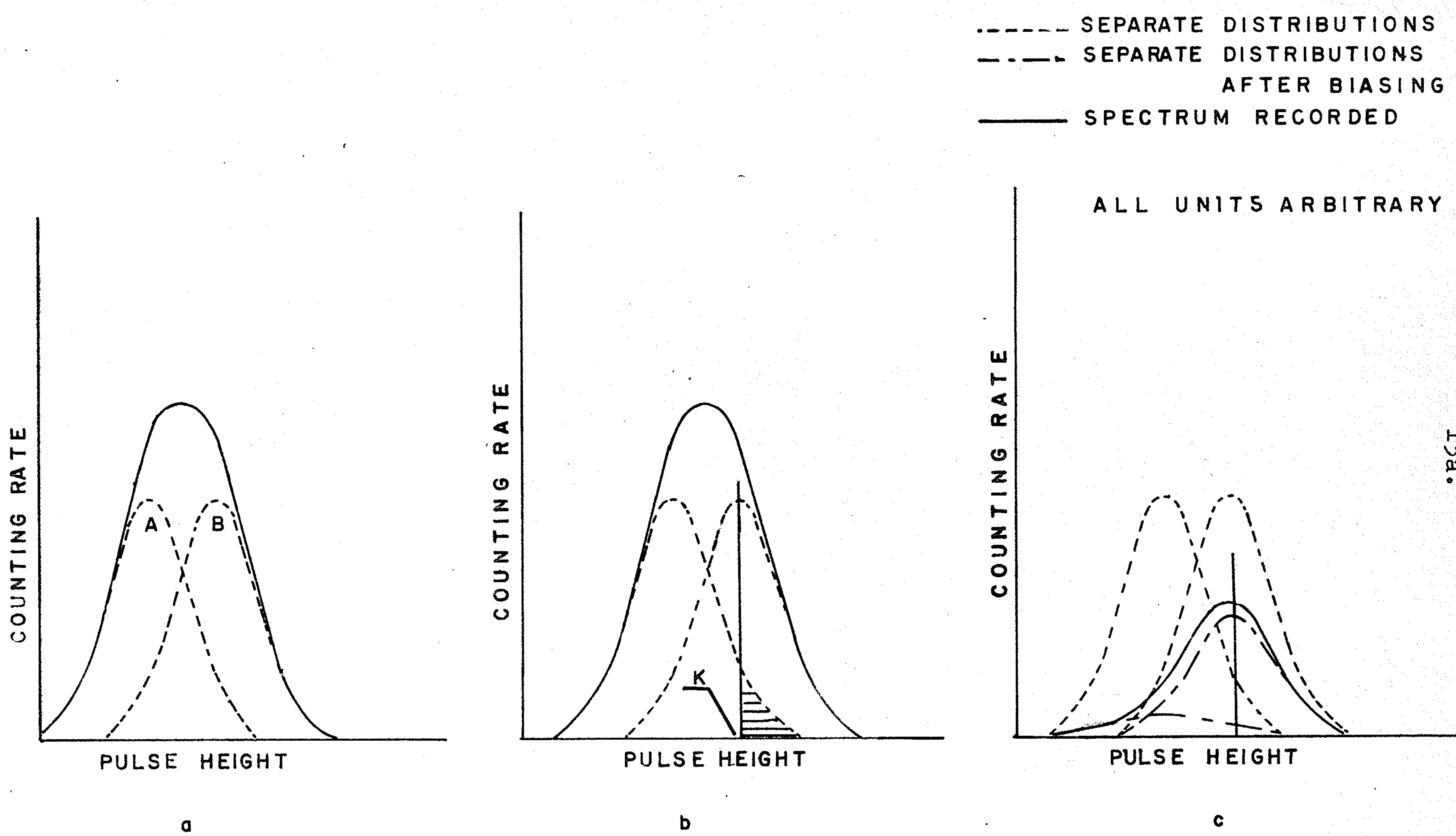
SEPARATE DISTRIBUTIONS
SEPARATE DISTRIBUTIONS AFTER BIASING
SPECTRUM RECORDED
ALL UNITS ARBITRARY
COUNTING RATE
PULSE HEIGHT
A
B
a
COUNTING RATE
PULSE HEIGHT
K
b
COUNTING RATE
PULSE HEIGHT
c

FIGURE 2

distribution A. The height of distribution A is therefore considerably reduced as is shown in Figure 2 (c). A similar argument applies to distribution B. However, this distribution, since it is centred about a higher pulse height than distribution A, will not be reduced to the same extent as distribution A. Figure 2 (c) also indicates the affect of the ''gating'' on distribution B. The spectrum recorded is the sum of the two reduced photopeaks. Distribution B, however, provides the main contribution to the recorded spectrum. The result is depected by the solid line in Figure 2 (c). The high energy peak is clearly resolved.

This method was used to resolve the elastic photopeaks. At small scattering angles the energy of the Compton gamma-rays is not much smaller than that of the elastic scattered gamma-rays. The high energy edge of the Compton photopeak overlaps with the much smaller elastic photopeak. However, the method discussed above can resolve the elastic photopeak, at least for a scattering angle of about 30°. Figure 3 is an example of the emergence of this photopeak from the Compton ''tail'' as the integral discriminator is moved to successively higher positions. The position of the integral discriminator, relative to the position of the direct radiation photopeak, is shown in the Figure. The dotted lines in Figure 3 are obtained by reflecting the trailing edges of the elastic photopeaks about the position of the direct radiation photopeak.

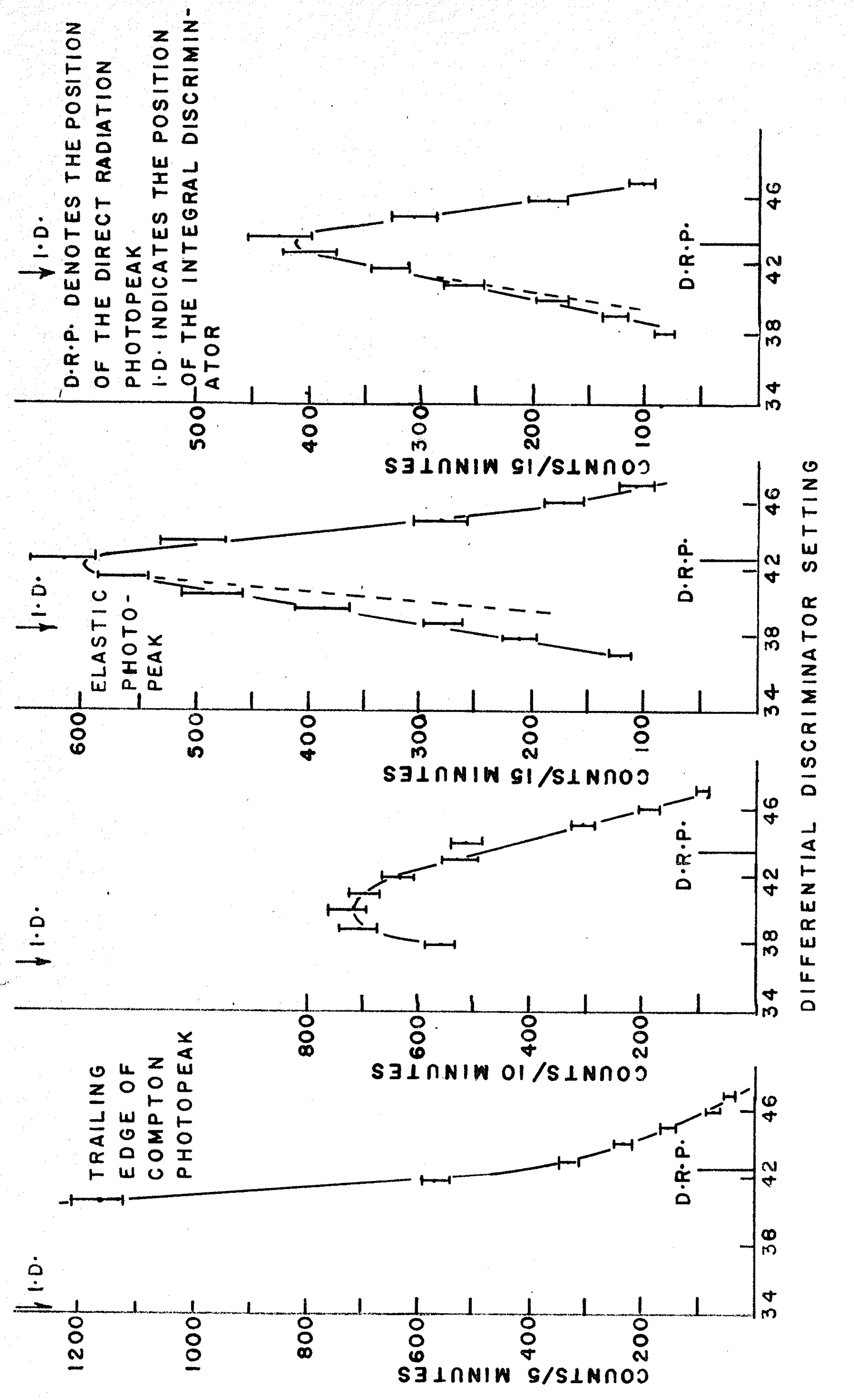
I·D·
D·R·P· DENOTES THE POSITION OF THE DIRECT RADIATION PHOTOPEAK
I·D· INDICATES THE POSITION OF THE INTEGRAL DISCRIMINATOR
ELASTIC PHOTO-PEAK
TRAILING EDGE OF COMPTON PHOTOPEAK
D·R·P·
COUNTS/5 MINUTES
COUNTS/10 MINUTES
COUNTS/15 MINUTES
DIFFERENTIAL DISCRIMINATOR SETTING

FIGURE 3·

A block diagram of the apparatus is given in Figure 4. A 1 5/8'' diameter X 2'' long Harshaw mounted NaI (Tl) crystal was used. The photomultipliers are 2'' DuMont 6292's. A good optical bond between photomultipliers and crystal was assured by using Dow Corning ''200'' fluid. Each photomultiplier output was fed to an Oak Ridge Model A1A preamplifier, and then to an Oak Ridge Model A1D linear pulse amplifier. On each amplifier chassis an integral discriminator was mounted. One of these integral discriminators was used, as is shown in Figure 4. The differential discriminator is a Type N/101 built by Dynatron Radio Limited. The coincidence unit is a Type 1036B built at Harwell. An Oak Ridge Model 201-B scaler (scale of 256) was used to count the coincidence output pulses.

It must be ensured that the coincidence mixer receives the coincidence channel outputs at the same time. This was done in the following manner. An oscilloscope was externally triggered by the output of one of the amplifiers. The position of the Channel No. 1 output pulses was noted on the grid. The output of Channel No. 2 was then displayed on the oscilloscope and the delay adjusted until it occurs at the same position on the grid. This procedure must be followed for every setting of the integral discriminator. A coincidence resolving time of 1 micro-second was used. The manner in which the equipment was actually employed is described in the next section.

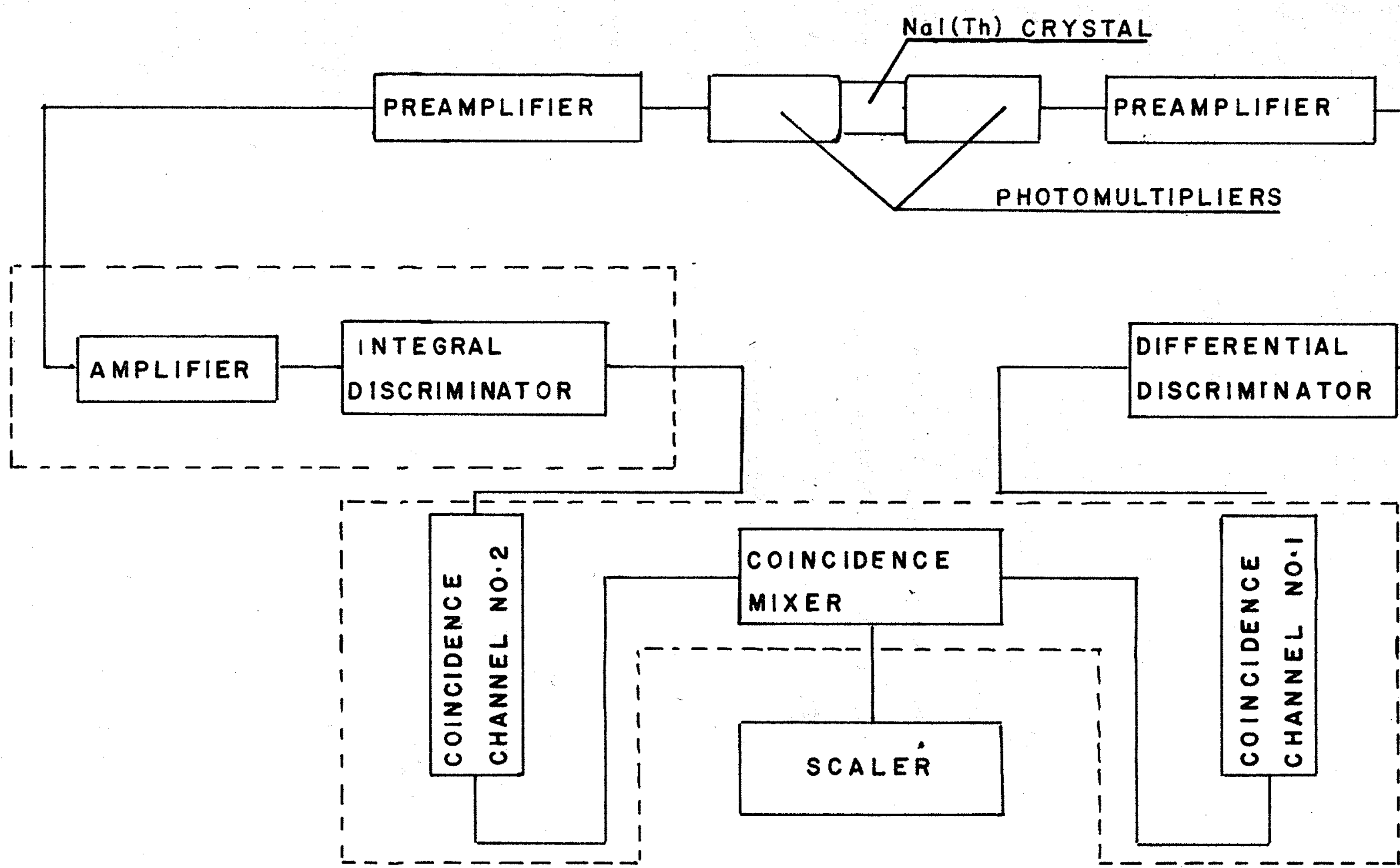
NaI(Th) CRYSTAL
PREAMPLIFIER
PREAMPLIFIER
PHOTOMULTIPLIERS
AMPLIFIER
INTEGRAL DISCRIMINATOR
DIFFERENTIAL DISCRIMINATOR
AMPLIFIER
COINCIDENCE CHANNEL NO·2
COINCIDENCE MIXER
COINCIDENCE CHANNEL NO·1
SCALER

FIGURE 4·

B. Experimental Method

Consider a scattering experiment in which N scattering centres†/cm.^{2} are deflecting gamma-rays from a source of strength s. In this experiment the number of counts per unit time recorded by a scintillation crystal is given by

$$n = \left(\frac{s}{4\pi}\right) \Omega_{ts} \left(\frac{d\sigma}{d\Omega}\right)_\theta N \, \Omega_{ct} \, \gamma \qquad \text{A}$$

with $\left(\frac{d\sigma}{d\Omega}\right)_\theta$ representing the differential cross section for the scattering angle θ, Ω_{ts} the solid angle subtended by the target at the source, Ω_{ct} the solid angle subtended by the crystal at the scattering centres and γ the detection efficiency of the crystal. Now suppose a point source of the same type but with strength $\bar{s}$ is placed at a position corresponding to the centre of the scatterer. The crystal is then subjected to the direct radiation from this source and

$$\bar{n} = \left(\frac{\bar{s}}{4\pi}\right) \Omega_{c\bar{s}} \, \gamma \qquad \text{A'}$$

predicts the counting rate. $\Omega_{c\bar{s}}$ is the solid angle subtended by the crystal at the source. This provides an equation for which, upon insertion into equation (A), yields

$$n = \left(\frac{s}{\bar{s}}\right) \bar{n} \left(\frac{d\sigma}{d\Omega}\right)_\theta N \, \Omega_{ts} \left(\frac{\Omega_{ct}}{\Omega_{c\bar{s}}}\right)$$

The differential scattering cross section is then given by

$$\left(\frac{d\sigma}{d\Omega}\right)_\theta = \left(\frac{n}{\bar{n}}\right) \left(\frac{\bar{s}}{s}\right) \frac{1}{N \, \Omega_{ts} \left(\frac{\Omega_{ct}}{\Omega_{c\bar{s}}}\right)}$$

---

† The number of scattering centres/cm.^{2} must be computed in a direction perpendicular to the incident beam.

It is therefore seen that a measurement of the source strength s is not required. The ratio of two source strengths will suffice for an absolute cross section measurement.

Since Ω_{ct} varies over the target surface, a more accurate expression is obtained by considering the target as subdivided into a number of equal sections and then summing the contributions from each of these sections. The formula then becomes

$$\left(\frac{d\sigma}{d\Omega}\right)_\theta = \left(\frac{n}{\bar{n}}\right)\left(\frac{\bar{s}}{s}\right)\frac{1}{N^{*}\sum_{i}\Omega^{i}_{ts}\left(\frac{\Omega^{i}_{ct}}{\Omega_{c\bar{s}}}\right)} \tag{8}$$

the letter "i" being used to label the sections. N^{*} denotes the number of scattering centres/cm.^{2} where the approximation is made that it is the same for each section.

The ratio of the two source strengths can be determined by employing the inverse square law. Knowing the weight of the target, its dimensions, the dimensions of the subdivisions, and the geometry of the scattering system N^{*} can be computed. The terms Ω^{i}_{ts} can also be computed.

Consider the terms $\left(\frac{\Omega^{i}_{ct}}{\Omega_{c\bar{s}}}\right)$. These are experimentally determined in the following manner. The standard position for the source $\bar{s}$ corresponds to the centre of the target. The number of counts/unit time in the photopeak of the direct radiation is obtained when the auxiliary source $\bar{s}$ is at a position corresponding to the centre of the i th segment. The ratio of these two counting rates is taken as the ratio $\left(\frac{\Omega^{i}_{ct}}{\Omega_{c\bar{s}}}\right)$. Since the solid angle $_{ct}$ varies slowly over the target surface a few segments will give a good approximation to the case where the number of segments approaches infinity.

The ratio $\left(\frac{n}{\bar{n}}\right)$ is obtained experimentally by using the following procedure. The integral discriminator is set to some position along the leading edge of the direct radiation photopeak. The differential discriminator, with a wide gate width, straddles this photopeak. The source s is blocked off and the source $\bar{s}$ placed at its standard position. The counting rate $\bar{n}$ is then determined. The source $\bar{s}$ is then removed and the other source unblocked. A suitable target is put in place and the counting rate obtained. When background is being taken the source is left in its position and an aluminium scatterer replaces the main scatterer. The aluminium target is chosen to have approximately the same number of electrons as the heavy target. The reason for employing the aluminium scatterer is that it will give approximately the same number of Compton and ''pile-up''† counts but will not give any appreciable†† elastic scattering. Subtracting the background from the heavy target counting rate gives some counting

---

† When two events occur within the resolving time of the system they register as a single event. The pulse height of the ''single'' event is the sum of the pulse heights of the two actual events. This phenomenon is termed ''pile-up''.

†† Under the conditions of the experiment reported in this thesis the ratio of the number of elastic scattered gamma-rays from lead to the number of elastic scattered gamma-rays from aluminium will be of the order of 10^5. This figure is based on Franz' formula and assumes that the two targets have approximately the same number of electrons.

rate n^*. This procedure is repeated for successively higher integral discriminator settings. Increasing the integral discriminator settings should decrease the contribution of the extraneous distributions (such as the bremsstrahlung and Compton scattering from bound electron distributions) to the counting rate n^* since it is expected that these distributions will decrease with increasing pulse height in the region of the elastic photopeak. The ratio $\left(\frac{n^*}{\bar{n}}\right)$ should therefore decrease and, it is hoped, approach some constant value. If a constant value is reached it will be the required ratio $\left(\frac{n}{\bar{n}}\right)$. This situation will be realized if the integral discriminator can be set past any distribution except a portion of the elastic scattering distribution. $\left(\frac{n^*}{\bar{n}}\right)$ is plotted against some function of the integral discriminator settings and if a constant value is reached $\left(\frac{n}{\bar{n}}\right)$ can be obtained.

To obtain the actual value of n a correction must be applied for target absorption. In computing the magnitude of this correction the experimental situation was idealized to a parallel beam striking the target and a parallel beam scattered at some angle . An absorption factor ''a'' was defined as follows:

$$a = \frac{\text{number of full energy gamma-rays absorbed / unit time}}{\text{number of elastically scattered gamma-rays/unit time assuming no absorption}}$$

Employing the above approximations the absorption coefficient is given by

$$a = 1 - e^{-\mu t \sec \phi}$$

where μ is the linear absorption coefficient for the target material, t is the target thickness and ϕ is the angle that the incident and scattered beams make with the horizontal. The experimental situation employed was such that the two beams are tilted at the same angle with respect to the horizontal. In order to check the accuracy of this correction two different target thicknesses were used.

Since all the factors in equation B (page 19) can be computed or measured† it is possible to make an absolute differential scattering cross section measurement for the elastic scattering of gamma-radiation. It was pointed out that a source strength measurement need not be made. The technique employed in an actual experiment has been discussed. The next section will discuss the results of the experiment performed.

---

† Experimentally it is found that $\left(\frac{\eta}{\lambda}\right)$ can be determined by the method described in the text.

IV RESULTS

This section reports the results of an experiment conducted in order to determine the differential elastic cross section for the scattering of 1.12 Mev. gamma-radiation by lead at an angle of $33^{\circ} \pm 4^{\circ}$ †. Two lead targets of different thicknesses were utilized. Absorption in the thick (9.29 ± 0.03 mm.) target resulted in a calculated loss of 51% of the elastic scattered gamma-rays. The thin (3.19 ± 0.01 mm.) target absorbed a calculated 21% of the elastic scattered gamma-rays. The differential scattering cross section obtained with the thick target was 23.3 ± 1.3 millibarns/steradian while the thin target yielded a result of 21.2 ± 1.4 millibarns/steradian. The errors quoted are the standard deviations (S.D.) of the counting rates.

Of crucial importance for the experiment was the determination of $\left(\frac{n}{\bar{n}}\right)$. This factor was obtained, for the two thicknesses, from the data presented in Figure 5. The abscissa is some function of the integral discriminator setting ††. The top set of points is for the thick scatterer, while the bottom set is for the thin scatterer. A straight line was fitted to

---

† One half of the angle subtended by the crystal at the centre of the target is taken as the uncertainty in the angle. The angle subtended by the target at the centre of the crystal is 8°.

†† The abscissa values were actually determined in the following manner. The integral discriminator was set at some very low value and the direct radiation photopeak was obtained. The integral discriminator was then set to the position at which n^{*} was to be measured, and the direct radiation photopeak again determined. The ratio of the photopeak heights in the two cases was taken as the abscissa value.

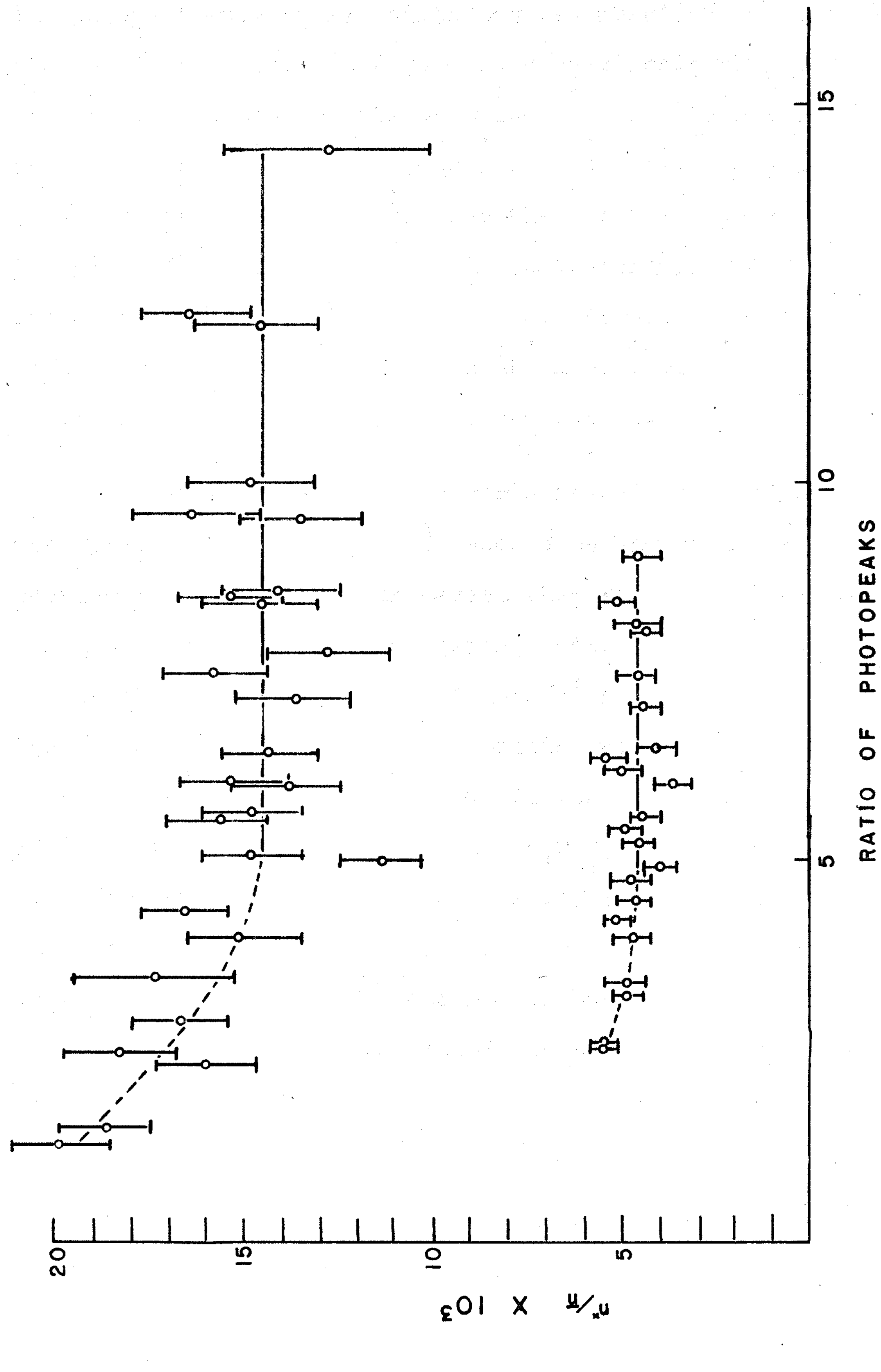

FIGURE 5.

each set of points by employing the method of least squares. Inclusion of only those points past an abscissa value of 5 yielded lines (shown in Figure 5) very closely parallel to the abscissa. The mean of the ordinates of all the points past the abscissa was then determined for each set and these means taken as the two $(\frac{n}{\bar{n}})$ values. For the thick scatterer $(\frac{n}{\bar{n}}) = 14.5$ ($\pm$ 2%) x 10^{-3} while for the thin scatterer $(\frac{n}{\bar{n}}) = 4.6$ ($\pm$ 3%) x 10^{-3}. These errors are counting rate (S.D.) errors. It is possible that a systematic error is present in each of these values due to an inaccurate correction for absorption.

If no appreciable error arises in correcting for absorption the factor $\frac{1}{N'}(\frac{n}{\bar{n}})$ should be the same for both scatterers. For the thick target this factor has the value $4.6 \pm 0.09 \times 10^{-22}$ cm.^{2}/scattering centre while for the thin target the value is $4.2 \pm 0.13 \times 10^{-22}$ cm.^{2}/scattering centre. These two figures do not agree within the standard deviations of the counting rates. Hence it is very probable that there is some significant error in the correction for absorption. Therefore only the thin target result will be accepted rather than the mean of the two results. However, the probable inaccurate correction for absorption may introduce a systematic error of the same order of magnitude as the total counting rate error (6.5%).

The ratio of the source strengths $(\frac{\bar{s}}{s})$ was determined by using the inverse square law. Since the two source strengths differ very greatly two intermediate sources[†] were employed in order that reasonable distances and counting rates could be used. In the actual procedure two distances, 113.1 ± 0.2 cms. and 364.7 ± 0.3 cms., were marked out from the centre of the top surface of a cylindrical (1 in. long x 1 in. diameter) NaI (Tl) crystal. The finite size of the crystal produces a small systematic error in these inverse square law measurements. In positioning the sources care was taken to place the centres of the sources[††] at these distances. The result obtained was $\frac{\bar{S}}{s} = 1.37 \times 10^{-3}$ with a 1.5% counting rate (S.D.) error.

The rather large source S introduces some uncertainty in the values of the solid angles subtended at the source by the various target segments. A rough estimate places the uncertainty in each solid angle computation at about 5%. The value used for the term $\sum_i \Omega^i_{ts}\left(\frac{\Omega^i_{ct}}{\Omega_{ci}}\right)$ was 2.7×10^{-2}, the standard deviation of the counting rates being 2%. Since a large number of segments (12 segments) were taken it is not expected that the large dimensions (5 cms. x 4 cms.) of the target will introduce an appreciable systematic error in the terms .

---

† Let the smaller intermediate source be S_1 and the larger intermediate source be S_2. The ratio $\left(\frac{\bar{S}}{s}\right)$ is then written in the form $\left(\bar{S}/s\right) = \left(\bar{S}/S_1\right)\left(\frac{S_1}{S_2}\right)\left(\frac{S_2}{s}\right)$ and the three ratios $\left(\frac{\bar{S}}{S_1}\right)$, $\left(\frac{S_1}{S_2}\right)$ and $\left(\frac{S_2}{s}\right)$ are experimentally determined.

†† The small source s and the auxiliary sources employed were all very small having dimensions of the order of 2 mms. However, the large source S was enclosed in a capsule (see Figure 1) whose length was about 3.5 cms. and whose maximum diameter was about 1.5 cms.

The counting rate error for the thick target is therefore 5.5% while for the thin target it is 6.5%. However, if systematic errors were included a reasonable estimate of the error would be about 20%. By employing a more localized source and thinner targets this error could be drastically reduced.

The experiment reported in this thesis therefore gives a differential cross section value of 21.2 ± 1.4 (S.D.) millibarns/steradian for the elastic scattering of 1.12 Mev. gamma-rays from lead at $33^{o} \pm 4^{o}$.

V DISCUSSION

The previous section reported a measurement which determined the differential cross section for the elastic scattering of 1.12 Mev. gamma-rays from lead at an angle of 33°. In this section the result obtained will be compared with the theoretically predicted results as well as with the results of other workers. Finally some comments will be made on the merits of the experimental method employed.

The experiment discussed in this thesis yielded 21.2 ± 1.4 millibarns/steradian as the differential cross section for the elastic scattering of 1.12 Mev. gamma-rays from lead at an angle of $33^{\circ} \pm 4^{\circ}$. Franz' form factor calculation (13) for Rayleigh scattering, combined with nuclear Thomson scattering, predicts a value of 18.2 millibarns/steradian. On the other hand Bethe's form factor calculation (14), combined with nuclear Thomson scattering, predicts a differential cross section of 41.7 millibarns/steradian. Although Bethe's computation involved only the K shell electrons the L shell electrons were taken into consideration by multiplying the form factor by 1.2. This correction should be valid for large changes in photon momentum (15) as is the case in the experiment reported in this thesis[†]. Further it is expected that for photon momentum changes larger than the characteristic momentum of a K electron the Bethe form factor computation should be better than Franz' calculation[††] (14). It is therefore slightly surprising

---

[†] In the experiment reported $\frac{\Delta q}{mc} = 1.25$

[††] For the experiment discussed in this thesis Δq was 2.08 times the characteristic momentum of a K electron.

that Franz' calculation is in better agreement with the experimental result. This may be due to an incorrect estimate of the contribution from the other electrons in the computation using Dirac wave functions.

Figure 6 displays the results of Mann (7), Eberhard and Goldzahl (6), and Wilson (4). The results of these workers are roughly consistent with each other. It is evident that for scattering angles of less than 60° the experimental data is in better agreement with Franz' computation rather than with Bethe's calculation. Point A on the graph represents the author's result. This point is for 1.12 Mev. radiation while the points representing the results of other workers are for 1.33 Mev. In order to compare this cross section with the cross sections of other workers compensation was made for the different energy by using the theoretical cross section[†]. The resulting value is plotted as point B. The cross section reported in this thesis is therefore consistent with data presented by other workers.

The advantages of the method reported in this thesis will now be discussed. Evidently, for a given statistical accuracy, results can be obtained much more quickly than by employing, say, Mann's method (7). Since Mann subtracts two curves which are almost the same (Compton tails for lead and aluminium scatterers) his counting times must be very long if the statistical accuracy is going to be reasonable. Also Mann

---

† Both Franz' and Bethe's form factor give approximately the same compensation factor.

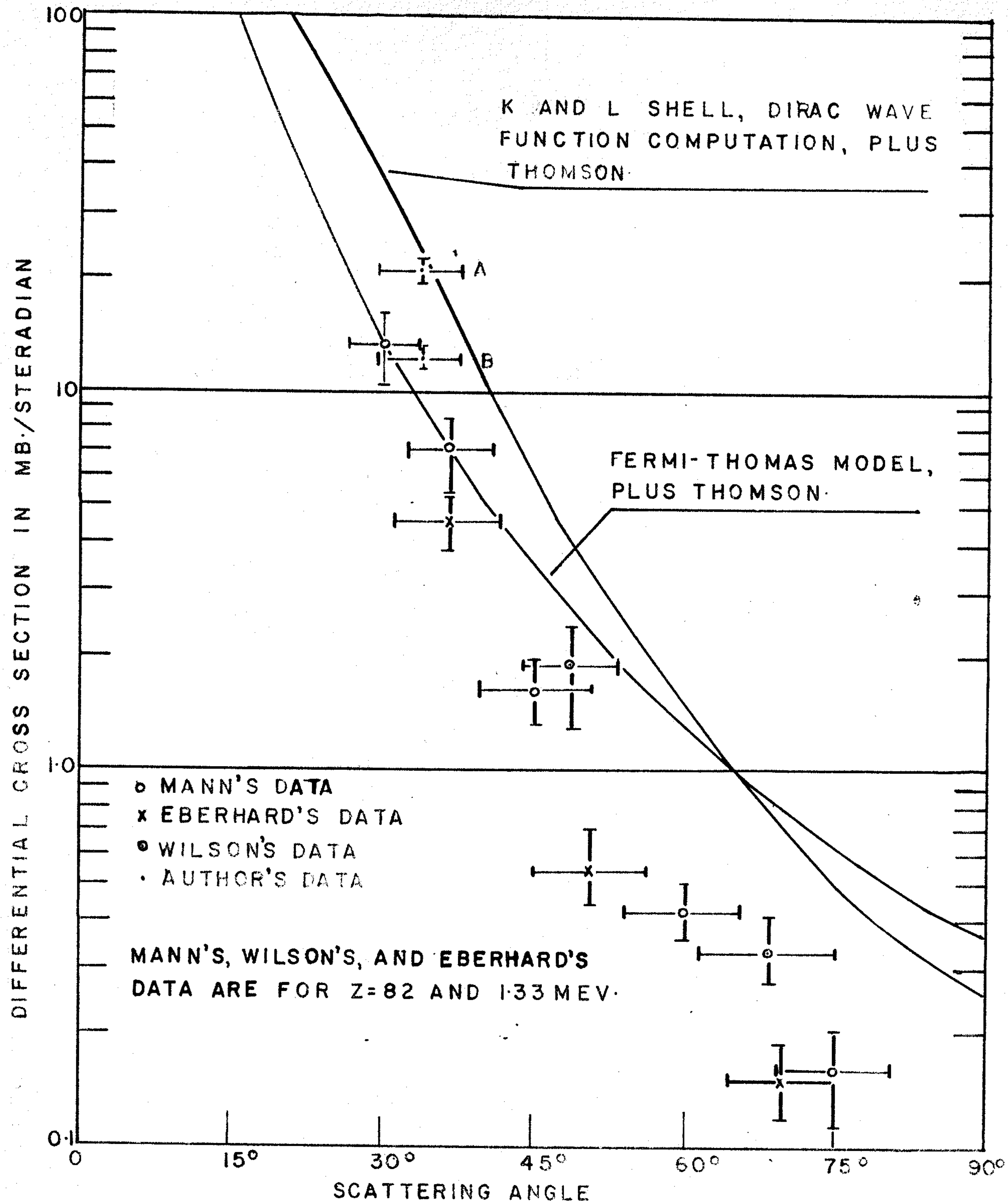
100
10
1·0
0·1
0
15°
30°
45°
60°
75°
90°
SCATTERING ANGLE
DIFFERENTIAL CROSS SECTION IN MB./STERADIAN
K AND L SHELL, DIRAC WAVE FUNCTION COMPUTATION, PLUS THOMSON.
FERMI-THOMAS MODEL, PLUS THOMSON.
A
B
o MANN'S DATA
x EBERHARD'S DATA
⊙ WILSON'S DATA
· AUTHOR'S DATA
MANN'S, WILSON'S, AND EBERHARD'S DATA ARE FOR Z=82 AND 1·33 MEV.

FIGURE 6.

still has the problem of another distribution (which he attributes to bremsstrahlung and Compton scattering by bound electrons) overlapping his elastic photopeak. Other workers, of course, experience the same difficulties as Mann. The troublesome distribution is eliminated in the method reported in this thesis.

The work done at 33^{o} indicates that the possibility of measuring the cross section of smaller scattering angles is very excellent. It is very likely that no great difficulties would be encountered down to scattering angles of about 15^{o}. Even if large angle scattering is being studied this method might be profitably employed. Distributions arising from such effects as bremsstrahlung caused by photoelectrons in the target and Compton scattering by bound electrons would be eliminated. Also if the source had some lower energy gamma-rays the contributions from these would be eliminated.

In conclusion this thesis has shown the efficacy of a particular method for measuring differential cross sections at small angles. The method discussed was employed to obtain the differential cross section for 1.12 Mev. gamma-rays scattered from lead at an angle of $33^{o} \pm 4^{o}$. The result reported was 21.2 ± 1.4 millibarns/steradian.

REFERENCES

(1) J.M. Jauch and F. Rohrlich,

The Theory of Photons and Electrons

Page 379 of 1st Edition.

(2) M. Delbruck,

Z. Physik 84, 144, 1933.

(3) R.R. Wilson,

Phys. Rev. 90, 720, 1953.

(4) W.G. Davey,

Proc. Phys. Soc. (Lond.) A66, 1059, 1953.

(5) L. Goldzahl and P. Eberhard,

Comptes Rendus 240, 965, 1955.

(6) A.K. Mann,

Phys. Rev. 101, 4, 1956.

(7) K.G. Standing and R.W. Peelle,

Rev. Sci. Inst. 24, No. 3, 193, 1953.

(8) C.M. Davisson and R.D. Evans,

Rev. Mod. Phys. 24, No. 2, 80, 1952.

(9) W. Heitler,

The Quantum Theory of Radiation (Oxford)

Page 219 of 3rd Edition.

(10) W. Heitler,

The Quantum Theory of Radiation (Oxford)

(11) W. Heitler,

The Quantum Theory of Radiation (Oxford)

Page 34 of 3rd Edition.

(12) A.T. Nelms and I. Oppenheim,
Jour. of Res. of N.B.S. 55, No. 1, 1955.

(13) W. Franz,
Z. Physik, 98, 314, 1936.

(14) J.S. Levinger,
Phys. Rev. 87, 656, 1952.

(15) G.E. Brown and J.B. Woodward,
Proc. Phys. Soc. A65, 977, 1952.

(16) P. Greifinger, J.S. Levinger and F. Rohrlich,
Phys. Rev. 87, 663, 1952.

(17) G.E. Brown, R.E. Peierls and J.B. Woodward,
Proc. Phys. Soc. A227, 51, 1954.

(18) S. Breuner, G.E. Brown, and J.B. Woodward,
Proc. Phys. Soc. A227, 59, 1954.

(19) P.B. Moon,
Proc. Phys. Soc. A63, 1189, 1950.

(20) J.S. Levinger,
Phys. Rev. 84, 523, 1951.

(21) W. Heitler,
The Quantum Theory of Radiation (Oxford)
Page 326 of 3rd Edition.

(22) R. Karplus and M. Neumann,
Phys. Rev. 83, 776, 1951.

(23) F. Rohrlich and R.L. Gluckstern,
Phys. Rev. 86, 1, 1952.

(24) J.S. Toll,
Thesis, Princeton University, 1952.

(25) H.A. Bethe and F. Rohrlich,
Phys. Rev. 86, 10, 1952.